PROTEINS
STRUCTURE ■ FUNCTION ■ BIOINFORMATICS

A Mg^{2+}-induced conformational switch rendering a competent DNA polymerase catalytic complex

Jesús Mendieta, Clara E. Cases-González, Tania Matamoros, Galo Ramírez, and Luis Menéndez-Arias*

Centro de Biología Molecular "Severo Ochoa," Consejo Superior de Investigaciones Científicas-Universidad Autónoma de Madrid, Cantoblanco, Madrid 28049, Spain

ABSTRACT

The structural and dynamical changes occurring before nucleotide addition were studied using molecular dynamics (MD) simulations of human immunodeficiency virus type 1 (HIV-1) reverse transcriptase (RT) complexes containing one or two Mg^{2+} ions in the presence of dNTP. Our models revealed that the formation of a catalytically competent DNA polymerase complex required subtle rearrangements at the catalytic site A, which occurred only when an Mg^{2+} ion was bound. This model has been validated using pre-steady-state kinetics to show that free Mg^{2+} is necessary to obtain a catalytically competent polymerase. Kinetic studies carried out with Be^{2+} as a cofactor permitted the functional discrimination between metal sites A and B. At low concentrations, Be^{2+} increased the catalytic efficiency of the polymerase, while at higher concentrations, it competed with Mg^{2+} for binding to site A, and inhibited DNA polymerization. In agreement with experimental data, MD simulations revealed that the catalytic attack distance between the 3′-OH of the primer and the α phosphorus in complexes containing Be^{2+} instead of Mg^{2+} at site A was above 4.5 Å. Our findings provide a detailed description of the mechanism of DNA polymerization and should be helpful to understand the molecular basis of DNA replication fidelity.

Proteins 2008; 71:565–574.

Key words: HIV; reverse transcriptase; catalytic ions; molecular dynamics; pre-steady-state kinetics; magnesium; beryllium.

INTRODUCTION

DNA polymerases play a fundamental role in the transmission and maintenance of genetic information. These enzymes copy a nucleic acid template by the stepwise addition of nucleotides onto the terminal 3′-OH of a DNA primer. On the basis of sequence homologies and crystal structure analysis, DNA polymerases have been grouped into various families, namely A, B, C, D, X, Y, and RT.[1,2] Despite their structural diversity, DNA polymerases share an overall morphology which includes a large nucleic acid-binding cleft comprised of three subdomains termed "fingers," "palm," and "thumb" by virtue of the similarity of the polymerase domain to the structure of a right hand.[3,4] The bottom of the cleft is formed by the "palm" subdomain, which harbors three catalytic residues that coordinate with two divalent ions.

All DNA polymerases are believed to use a common "two-metal ion" mechanism for nucleotidyl transfer, which was proposed by analogy to the nearly identical mechanism of the 3′-5′ exonuclease of DNA polymerase I.[5,6] In this mechanism, the 3′-OH group at the end of the DNA strand attacks the α-phosphate of the incoming dNTP to form a new phosphodiester bond with the subsequent release of pyrophosphate. The two metal ions found in the DNA polymerase active site (usually two Mg^{2+} ions) are separated by ~4 Å and roughly in line with the phosphor–sugar backbone on the opposite site of the bases. The catalytic metal (metal A) is thought to lower the pK_a of the 3′-OH of the growing primer terminus (nucleophile formation), while the nucleotide binding metal (metal B) coordinates the triphosphate moiety and facilitates pyrophosphate dissociation. Both metals are believed to stabilize the proposed penta-coordinated transition state of the nucleotidyl transferase reaction. Although Mg^{2+} is probably the divalent metal ion utilized by most polymerases for catalysis *in vivo*, DNA polymerases are able to use other divalent cations, in particular Mn^{2+}. However, divalent cations such as Mn^{2+}, Ni^{2+}, Co^{2+},

The Supplementary Material referred to in this article can be found online at http://www.interscience.wiley.com/jpages/0887–3585/suppmat.

Grant sponsor: Spanish Ministry of Education and Science; Grant number: BIO2003/01175; Grant sponsor: Fundación Ramón Areces (Centro de Biología Molecular "Severo Ochoa")

*Correspondence to: Luis Menéndez-Arias, Centro de Biología Molecular "Severo Ochoa", Consejo Superior de Investigaciones Científicas-Universidad Autónoma de Madrid, Cantoblanco, Madrid 28049, Spain.
E-mail: lmenendez@cbm.uam.es

Received 19 April 2007; Accepted 29 June 2007
Published online 26 October 2007 in Wiley InterScience (www.interscience.wiley.com). DOI: 10.1002/prot.21711

and Be^{2+} are known to alter the nucleotide selectivity and fidelity of DNA synthesis in reactions catalyzed by several DNA polymerases.[7–10]

Crystal structures of ternary complexes containing the DNA polymerase, a template-primer, and an incoming dNTP are available for polymerases belonging to families A, B, X, Y, and RT and have provided valuable information on the geometric arrangement of the essential divalent cations.[11] Evidence of the coordination of the 3′-OH primer terminus by the catalytic Mg^{2+} has been recently reported for a DNA polymerase β (family X) ternary complex obtained using a non-hydrolyzable dUTP analog.[11] However, in most cases, a structural insight into the catalytic mechanism has been hampered by the lack of the 3′-OH or the catalytic Mg^{2+}.

Conformational changes triggered by the occupation of the metal sites A or B, and occurring before chemical bond formation, are expected to play an important role in enhancing the polymerase fidelity by an induced-fit mechanism.[12,13] Functional dissection of the roles of the two metal ions is difficult, although the conformational changes occurring during the polymerization reaction pathway have been followed in stopped-flow tryptophan fluorescence assays, using DNA polymerase β complexed with double-stranded DNA and Rh^{3+}/dCTP.[14] These studies demonstrated that the limiting step of the nucleotide incorporation reaction occurred after addition of the catalytic Mg^{2+} (site A).[14]

In this work, we have used molecular dynamics (MD) simulations to delineate the structural and dynamical changes that occur before the nucleotidyl transfer reaction, and the conformational motions related with the occupancy of metal sites A and B, based on the structure of a ternary complex of human immunodeficiency virus type 1 (HIV-1) reverse transcriptase (RT), double-stranded DNA, and dTTP.[15] Pre-steady-state kinetic experiments showed that the presence of the catalytic Mg^{2+} (site A) is required to obtain a catalytically competent HIV-1 RT complex. However, beryllium whose mutagenic effects have been previously reported for the homologous avian myeloblastosis virus RT,[7,16] has a dual effect. At relatively low concentrations (micromolar range), Be^{2+} ions increase the catalytic efficiency of the RT's polymerase activity, while at higher concentrations, they compete with Mg^{2+} for binding to metal site A, inhibiting DNA polymerization.

EXPERIMENTAL PROCEDURES

Stock solutions of dTTP (100 m*M*) and [γ-^{32}P]ATP were obtained from GE Healthcare. Synthetic DNA oligonucleotides 21P (5′-ATACTTTAACCATATGTATCC-3′) and 31T (5′-TTTTTTTTTAGGATACATATGGTTAAAGTAT-3′) were obtained from Life Technologies. The oligonucleotide 21P was labeled at its 5′ terminus with [γ-^{32}P]ATP and T4 polynucleotide kinase (New England Biolabs) and then annealed to 31T to obtain the template-primer substrate to be used in kinetic assays. $BeSO_4$ was obtained from BDH Laboratory Supplies (Poole, UK). All other reagents, including $MgCl_2$ and $MgSO_4$, were purchased from Merck or Sigma.

RT expression and purification

Recombinant heterodimeric HIV-1 RT (strain BH10) was expressed and purified using a modified version of plasmid p66RTB, as previously described.[17,18] The wild-type RT was coexpressed with HIV-1 protease in *E. coli* XL1 Blue to get p66/p51 heterodimers, which were later purified by ionic exchange followed by affinity chromatography. Enzymes were quantified by active site titration[19,20] before biochemical studies.

Pre-steady-state kinetic assays

Pre-steady-state kinetic parameters for the incorporation of dTTP were determined with a rapid quench instrument (model QFM-400, Bio-Logic Science Instruments, Claix, France) with reaction times ranging from 10 to 6000 ms. Reactions were preformed by mixing 12 μL of a solution containing 40–50 n*M* (active sites) of HIV-1 RT and 100 n*M* of the template-primer 31T/21P in RT buffer (50 m*M* Tris-HCl, pH 8.0; 50 m*M* KCl) with 12 μL of RT buffer containing variable amounts of dNTP, Be^{2+}, or Mg^{2+}, depending on the experiment, and then quenched with 0.3*M* EDTA (final concentration). The reaction products were separated on a 20% (w/v) polyacrylamide/8*M* urea gel, and quantified by phosphorimaging with a BAS 1500 scanner (Fuji) using the program Tina version 2.09 (Raytest Isotopenmessgerate Gmbh, Staubenhardt, Germany). The formation of product [*P*] over time was fitted with a burst equation:

$$[P] = A \times [1 - \exp(-k_{obs} \times t)] + k_{ss} \times t$$

where A is the amplitude of the burst, k_{obs} is the apparent kinetic constant of formation of the phosphodiester bond, and k_{ss} is the enzyme turnover rate, that is the kinetic constant of the steady-state linear phase. The dependence of k_{obs} on dNTP concentration is described by the hyperbolic equation:

$$k_{obs} = k_{pol} \times [\text{dNTP}]/(K_d + [\text{dNTP}])$$

where K_d and k_{pol} are the equilibrium constant and the catalytic rate constant of the dNTP for RT, respectively. K_d and k_{pol} were determined from curve-fitting using SigmaPlot.

MD simulations

Simulations were performed using the SANDER module of AMBER 8 and the parm99 parameter set.[21] The

system used in the MD simulations was based on the X-ray structure determined by Huang *et al.*[15] (PDB code 1RTD). The system included the DNA polymerase domain (residues 1–390) of the 66 kDa-subunit of HIV-1 RT, a 15/12-mer DNA/DNA template-primer and residues 3–82 of the 51-kDa subunit of the RT. One or two Mg^{2+} ions and the incoming dTTP were also included in the system. Atomic charges for dTTP were obtained with the RESP program[22] to fit potentials calculated at 6-31G* level using the Gaussian-98 package.[23] In some MD simulations, magnesium cations in the A and/or B sites were replaced by Be^{2+}. Nonbonding parameters for this ion were adjusted in order to reproduce the geometry and the distances of the coordination sphere described by Pavlov *et al.*[24] An appropriate number of Na^{+} ions were added to neutralize the negative net charge of the system. The counterions and the solvent were added using the LEAP module of AMBER. Initial relaxation of each complex was achieved by performing 10,000 steps of energy minimization using a cut-off of 10.0 Å. Subsequently, and to start the MD simulations, the temperature was raised from 0 to 298°K in a 200-ps heating phase, and velocities were reassigned at each new temperature according to a Maxwell-Boltzmann distribution. During this period, the positions of the C_α atoms of the solute were restrained with a force constant of 20 kcal mol^{-1}. In a second phase, lasting 100 ps, the force constant was reduced stepwise. Finally, the system was allowed to relax during 100 ps restraining only the distance corresponding to the Watson–Crick hydrogen bonds between the first and the last base pairs of the DNA molecule and a positional restrain of the C_α of the p51 fragment, with a force constant of 10 kcal mol^{-1}. These constraints were maintained during all productive MD simulations. The SHAKE algorithm was used throughout to constrain all bonds involving hydrogens to their equilibrium values, so that an integration time step of 2 fs could be employed. The list of nonbonded pairs was updated every 25 steps, and coordinates were saved every 2 ps. Periodic boundary conditions were applied and electrostatic interactions were represented using the smooth particle mesh Ewald method with a grid spacing of ~1 Å. The trajectory length was 10 ns for all the complexes. Analysis of the trajectories was performed using the CARNAL module of AMBER 8.

RESULTS

MD-supported modeling of HIV-1 RT ternary complexes in the presence of one or two Mg^{2+} ions

The X-ray crystal structure of the ternary complex of HIV-1 RT, a dideoxyguanosine-terminated primer-template, and dTTP has revealed that two Mg^{2+} ions bind to the substrates and the active site residues. One Mg^{2+} is located at the dNTP binding site where it binds to nonbridging oxygen atoms of each of the phosphates of the incoming dNTP, a backbone carbonyl (Val-111), and the carboxylates of Asp-110 and Asp-185. The second Mg^{2+}, which would contact the 3′-OH of the primer, showed lower occupancy due to the missing hydroxyl group.[15]

The structural and dynamical changes occurring before the nucleotidyl transfer reaction were studied using MD simulations of the ternary complexes containing one or two Mg^{2+} ions, in the presence of dNTP. In the simulations we introduced a 3′-OH group at the blocked primer. The motion of the polymerase domain was followed over the 10.0-ns trajectory. In addition, MD simulations were carried out with the binary complex containing the RT and a DNA/DNA template-primer, in order to verify whether the opening of the subdomains occurred within the time scale of the simulations.

The root-mean-square deviations (rmsd) corresponding to the backbone C_α atoms of the ternary complex containing two Mg^{2+} ions remained below 1.7 Å, suggesting few conformational changes during all the simulation time [Fig. 1(A)]. However, the complex lacking the catalytic Mg^{2+} (site A) showed higher rmsd values (increasing up to 2.5 Å), and the rmsd values for the binary complex increased above 3.0 Å. The low rmsd values obtained when either the "palm" and "thumb" subdomains or the "fingers" subdomain were considered independently suggested that the conformational changes observed in the absence of the catalytic Mg^{2+} were consistent with a hinge-bending motion of the "thumb" subdomain relative to the "fingers" subdomain. However, this motion was not homogeneously distributed within the "fingers" subdomain. A large conformational change affects the β3-β4 hairpin loop (residues 56–77) after binding the Mg^{2+}/dNTP substrate. Thus, the distance between the tip of the β3-β4 hairpin loop (C_α atom of Lys-66) and the tip of the "thumb" subdomain (C_α atom of Leu-289) was in the range of 30–35 Å, in simulations carried out with the RT/DNA binary complex. In contrast, this distance was reduced to approximately 25 Å in simulated ternary complexes containing one or two Mg^{2+} ions [Fig. 1(B)]. The relative positions of the β3-β4 hairpin loop were similar in the presence of one or two Mg^{2+} ions.

In agreement with the observations referred above, the comparison of the C_α traces of the DNA polymerase domain showed significant changes in the relative distances and angles between "thumb" and "fingers" subdomains, which affected mainly to the conformation of the so-called β3-β4 hairpin loop (Fig. 2). The structure obtained from the MD simulation with the binary complex of HIV-1 RT and DNA showed an rmsd of 2.5 Å, when compared with the reported crystal structure.[25] On the other hand, the rmsd obtained from the super-

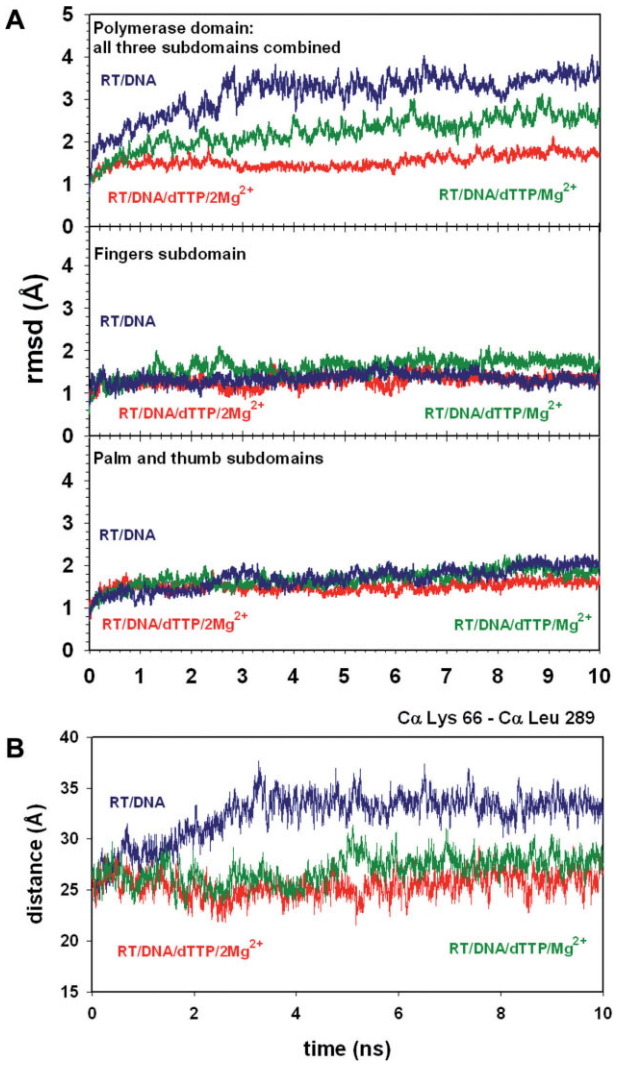

Figure 1

*Monitoring the conformational changes occurring upon binding of the catalytic Mg^{2+} along the simulation time. (**A**) Evolution of the rmsd of the C_α atoms of the polymerase domain (top), the "fingers" subdomain (middle), and "palm" and "thumb" subdomains together (bottom) in the simulated structures with respect to the crystal structure of the ternary complex HIV-1 RT/DNA/dTTP. (**B**) Relative increase of the interatomic distances between the C_α atoms of Lys-66 and Leu-289, in comparison with the initial distance measured in the crystal of the ternary complex. Lys-66 and Leu-289 are located in the tips of the β3-β4 hairpin loop (within the "fingers" subdomain), and "thumb" subdomain, respectively. For all panels, the data obtained with the structures containing one and two Mg^{2+} ions are indicated in green and red, respectively, while the binary complex of HIV-1 RT/DNA is shown in blue.*

position of the simulated ternary complex of HIV-1 RT, double-stranded DNA, dNTP, and two Mg^{2+} ions, and the crystal structure of the ternary complex reported by Huang *et al.*[15] was 1.75 Å. Ternary complexes obtained in the absence of the catalytic Mg^{2+} showed a less opened conformation than in the crystal structure of the binary complex.[25] These results are consistent with previous work showing that Mg^{2+} plays a critical role in the closing of the catalytic subdomains of DNA polymerase β.[26]

At the end of the simulation, interactions in the catalytic site of the ternary complex containing two Mg^{2+} ions were similar to those observed in the crystal structure (Fig. 3). Thus, the octahedral coordination shell of the catalytic Mg^{2+} involved its interaction with the 3′-OH of the primer, as well as with the carboxylates of Asp-110, Asp-185, and Asp-186, a nonbridging oxygen of the α-phosphate of dNTP, and a water molecule (Supplementary Table S1). The complex lacking the catalytic Mg^{2+} showed a more opened conformation but the coordination sphere of the Mg^{2+} in site B was almost identical to that observed in the same site when both Mg^{2+} ions were present. In the complex containing two Mg^{2+} ions, the most remarkable consequence of the incorporation of the 3′-OH group of the primer in the coordination shell of the catalytic Mg^{2+} is the significant decrease of the catalytic attack distance, that goes down to around 3 Å, thereby favoring the nucleotidyl transfer reaction. This reduction occurs within the first 0.5 ns of the simulation, while in the case of the

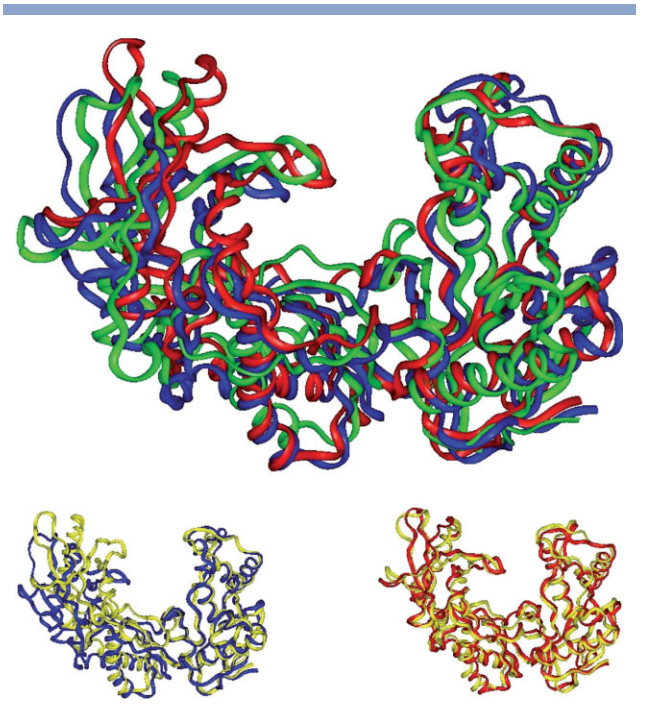

Figure 2

C_α traces of superimposed polymerase domains of the HIV-1 RT obtained from the MD simulations. The colored ribbons blue, green, and red indicate the simulated RT/DNA complexes with no Mg^{2+}, the nucleotide-binding Mg^{2+}, or with both Mg^{2+}, respectively. Superimpositions of the simulated RT/DNA binary complex with the crystal structure reported by Ding et al.[25] (left), and the simulated ternary complex containing two Mg^{2+} ions and the crystal structure reported by Huang et al.[15] (right) are shown below.

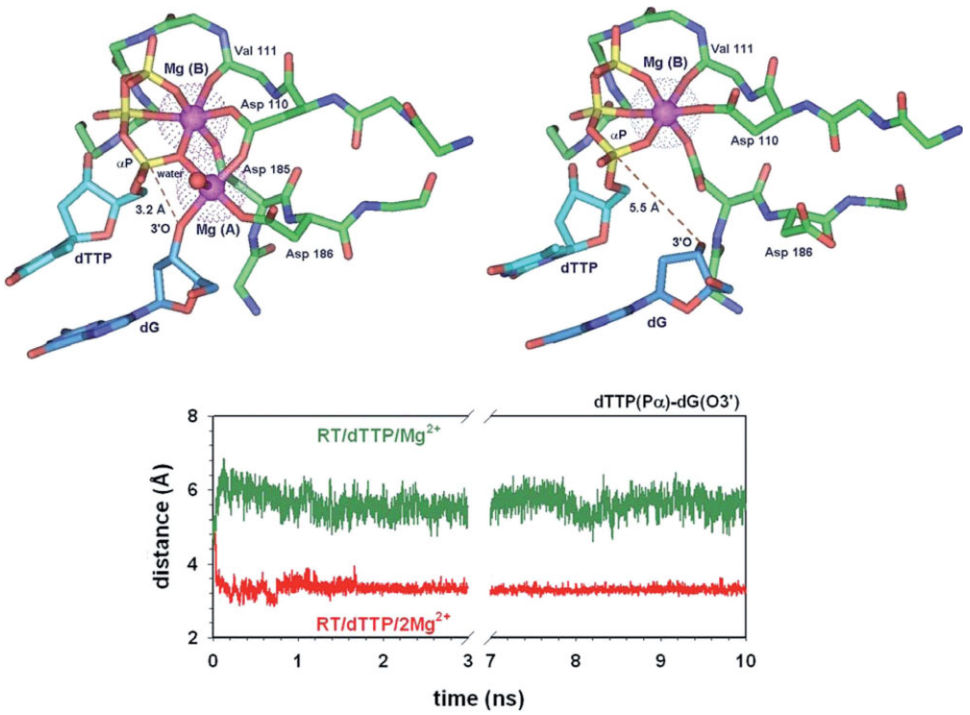

Figure 3

Detailed view of the positions of the bound Mg^{2+} ions in the energy-minimized average structures of the polymerase domain of HIV-1 RT in the presence of one or two metal ions in their active site. The evolution of the active site interatomic distances between the 3′O of the primer and the α phosphorus of the incoming dTTP in the two simulations are shown below.

complex lacking the catalytic Mg^{2+}, the distance increases above 6 Å (Fig. 3). Interestingly, stable hydrogen bonds are established between the incoming dNTP and the templating base upon incorporation of the Mg^{2+}/dTTP substrate (Supplementary Fig. S1), suggesting that this step is an important fidelity checkpoint in DNA polymerization.

On the basis of the results of the MD simulations, we propose that the DNA polymerization reaction pathway involves the initial binding of Mg^{2+}/dNTP to the polymerase–DNA binary complex. This step produces a "fingers" subdomain closing motion that involves a large conformational change affecting the β3-β4 hairpin loop and leads to additional rearrangements within the polymerase catalytic site. However, binding of free Mg^{2+} in metal site A stabilizes the formation of the competent DNA polymerase catalytic complex. MD simulations suggest that this step produces further local rearrangements of the catalytic site, while decreasing the catalytic attack distance. This model which is consistent with the hypothetical reaction pathway proposed by Joyce and Benkovic,[13] has been further validated using pre-steady-state kinetics to show the requirement of free Mg^{2+} to render a competent DNA polymerase catalytic complex, and the functional discrimination between metal sites A and B.

Single nucleotide incorporation kinetics in the presence of Mg^{2+}

Pre-steady state kinetic analysis of the incorporation of a single nucleotide by HIV-1 RT was carried out in the presence of 2 m*M* Mg^{2+}, under conditions where the DNA concentration was in excess relative to the RT concentration. As expected, the time courses obtained at different dNTP concentrations showed a burst of incorporation followed by a linear phase.[19] The corresponding burst rates were then plotted against [dNTP], and the data were fit to the hyperbolic equation $k_{obs} = k_{pol}[dNTP]/([dNTP] + K_d)$, where k_{pol} is the maximum rate of polymerization, and K_d is the equilibrium dissociation constant for dNTP. The obtained k_{pol} and K_d values were 11.6 ± 0.5 s^{-1} and 13.4 ± 1.9 μ*M*, respectively. Under our assay conditions, the active enzyme (i.e. catalytically competent RT polymerase complex) concentration can be determined from the pre-steady state burst amplitudes. In the presence of saturating concentrations of dNTP, burst amplitudes depend on the concentration

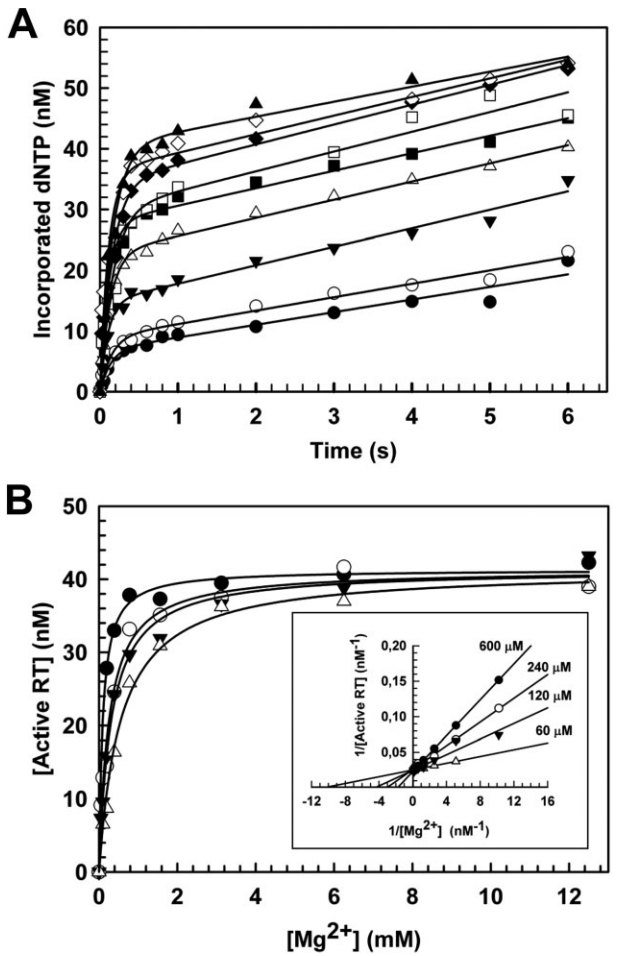

Figure 4

*Dependence of the Mg^{2+} dissociation constant on dNTP concentration. (**A**) Kinetic curves of incorporation of nucleotide in the presence of different concentrations of Mg^{2+}. A preincubated solution of RT (40 nM) plus template/primer 31T/21P (100 nM) was mixed with increasing concentrations of Mg^{2+} (0.05, 0.098, 0.195, 0.39, 0.78, 1.56, 3.125, 6.25, and 12.5 mM) in the presence of 240 µM dTTP, using a rapid chemical quench flow instrument. Reactions were quenched with EDTA at the indicated times and analyzed by polyacrylamide/urea gel electrophoresis. The solid lines represent the best fit of the data to a burst equation. The amplitudes (A) and the observed first-order rate constants for the burst phase (k_{obs}) were: 40.32 ± 1.34 nM, and 6.14 ± 0.64 s^{-1}, respectively, for 12.5 mM Mg^{2+} (▲); A = 36.25 ± 1.58 nM, and k_{obs} = 9.09 ± 1.47 s^{-1}, for 6.25 mM Mg^{2+} (◇); A = 34.17 ± 1.24 nM, and k_{obs} = 6.43 ± 0.75 s^{-1}, for 3.125 mM Mg^{2+} (◆); A = 29.77 ± 1.71 nM, and k_{obs} = 5.89 ± 1.05 s^{-1}, for 1.56 mM Mg^{2+} (□); A = 27.73 ± 0.73 nM, and k_{obs} = 8.91 ± 0.85 s^{-1}, for 0.78 mM Mg^{2+} (■); A = 22.62 ± 0.40 nM, and k_{obs} = 7.74 ± 0.47 s^{-1}, for 0.39 mM Mg^{2+} (△); A = 14.76 ± 0.54 nM, and k_{obs} = 9.65 ± 1.32 s^{-1}, for 0.195 mM Mg^{2+} (▼;); A = 8.93 ± 0.48 nM, and k_{obs} = 6.84 ± 1.23 s^{-1}, for 0.098 mM Mg^{2+} (○); and A = 6.87 ± 0.62 nM, and k_{obs} = 7.27 ± 2.22 s^{-1}, for 0.05 mM Mg^{2+} (●). (**B**) Inhibition of the formation of the catalytically competent RT polymerase complex due to Mg^{2+} chelation by dNTP. The concentration of active polymerase ([RT/DNA/dNTP·Mg^{2+}/Mg^{2+}]) was determined from the burst amplitudes of incorporation reactions (A) carried out at different concentrations of Mg^{2+}, in the presence of dNTP at 60 µM (△), 120 µM (▼), 240 µM (○), and 600 µM (●). Apparent K_d values obtained for Mg^{2+} binding in the presence of 60, 120, 240, and 600 µM dNTP were 95.7 ± 6.4 µM, 254.9 ± 33.3 µM, 309.3 ± 33.6 µM, and 553.6 ± 48.5 µM, respectively. Inset: Double-reciprocal plot of the data.*

of Mg^{2+} [Fig. 4(A)]. However, nucleotide substrates have a chelating effect on the reaction, and therefore, the amount of magnesium required to obtain the largest burst amplitudes was higher in the presence of relatively high dTTP concentrations [Fig. 4(B)]. Double reciprocal plots of the concentration of catalytically competent RT polymerase complex versus Mg^{2+} concentration, confirmed that the dNTP competes with the enzyme for binding free Mg^{2+} ions (i.e. the nucleotide substrates had a chelating effect on the reaction). A theoretical binding constant for Mg^{2+} (K_d = 0.218 ± 0.032 m*M*) was determined from the data shown in Figure 4(B), by extrapolating the data to conditions where the [dNTP] equals zero. The obtained K_d was similar to that reported for Mg^{2+} binding to ATP (K_d = 0.089 m*M*).[27,28]

Pre-steady-state kinetics and modeling studies using Be^{2+} as cofactor of the polymerization reaction

Although differences between sites A and B can be inferred from the results described earlier, functional distinction between both sites in the HIV-1 RT has remained so far elusive. Since Be^{2+} is a weak inhibitor of the DNA polymerase activity in the presence of Mg^{2+},[16,29] we performed MD simulations where Be^{2+} substituted for Mg^{2+} occupying metal sites A and/or B. Be^{2+} ions bind nucleoside-triphosphates with a three orders of magnitude higher affinity than Mg^{2+} (K_d = 2.4 × 10^{-8} *M*).[30] Therefore, we can assume that a ternary complex including Be^{2+} in metal site B and Mg^{2+} in metal site A would appear in the presence of Mg^{2+}, when [Be^{2+}] ≤ [dNTP]. However, when [Be^{2+}] > [dNTP], Be^{2+} can replace Mg^{2+} in metal site A, rendering a ternary complex where both metal sites are occupied by Be^{2+}. MD simulations for ternary complexes containing Mg^{2+} in site B and Be^{2+} in site A were also carried out, although these complexes may not occur in nature.

Unlike Mg^{2+}, the small Be^{2+} ions form bonds to oxygen atoms with substantial covalent character and with a strong tendency to achieve its maximum coordination number of 4. The structure of the catalytic site at the end of the MD simulations (Fig. 5) shows that when substituting Be^{2+} for Mg^{2+} in the ternary complex at site A, Be^{2+} coordinates with carboxylates of Asp-110, Asp-185, and Asp-186, as well as with a water molecule. The coordination geometry at site B is different depending on whether site A is occupied by Be^{2+} or Mg^{2+}. When Be^{2+} is found at both sites A and B, the nonbridging oxygen atoms of each of the phosphates of the incoming dNTP and the side chain of Asp-185 are coordinated with the cation. However, when a Mg^{2+} ion is present in site A, interactions at site B are rather different, with Be^{2+} coordinating with the nonbridging oxygens of the β,γ-phosphates, a carboxylate group of Asp-110, and the backbone carbonyl (Val-111). The coordina-

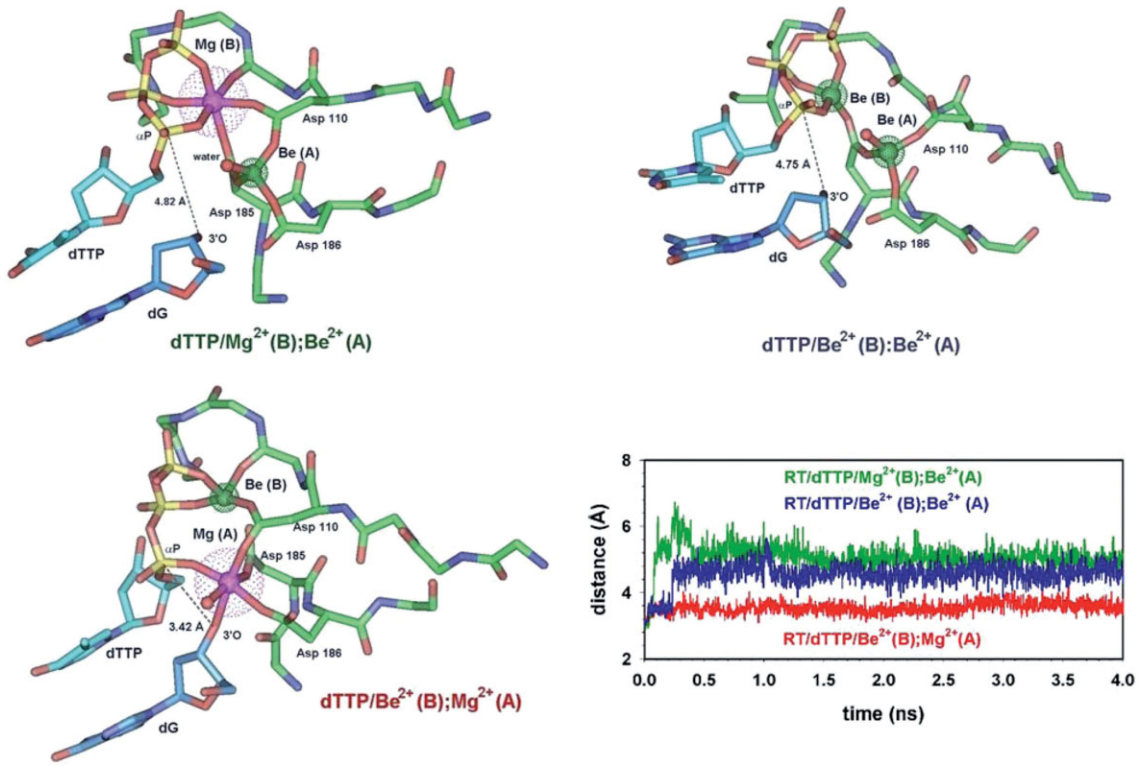

Figure 5

Detailed view of the active site of the HIV-1 RT in simulated ternary complexes containing Be^{2+} ions in metal sites A, B, or both. The evolution of the active site interatomic distances between the 3′O of the primer and the α phosphorus of the incoming dTTP in the three simulations are shown below.

tion between the catalytic metal and both the 3′-OH of the primer terminus and the nonbridging oxygen of the α-phosphate of the incoming dNTP appear to be critical to maintain the appropriate distance for the nucleophilic attack, and therefore to maintain the integrity of the catalytically competent DNA polymerase complex. The catalytic attack distance was around 3 Å only when the ternary complex contained Be^{2+} in metal site B and Mg^{2+} in metal site A (Fig. 5), suggesting that under these conditions the nucleotidyl transfer reaction could take place. These results were consistent with previous reports showing that in the absence of Mg^{2+}, RTs were devoid of DNA polymerase activity in the presence of variable amounts of Be^{2+}.[7]

Table I

Pre-Steady State Single-Nucleotide Incorporation Rate of the Reaction (k_{obs}) at Different Concentrations of Be^{2+}

$[Be^{2+}]$ (μ*M*)	k_{obs} (s^{-1})
0	9.92 ± 0.43
1.35	8.93 ± 0.81
5.4	18.43 ± 1.68
21.7	13.77 ± 1.53
86.7	14.98 ± 1.74
347	8.71 ± 0.62
1387	5.32 ± 0.46
5550	<0.5

A preincubated solution of RT (40 n*M*) plus template/primer 31T/21P (100 n*M*) was mixed with increasing concentrations of Be^{2+} in the presence of 100 μ*M* dTTP and 2 m*M* Mg^{2+}. Reactions were allowed to proceed for various time intervals and the incorporation rates were obtained with the corresponding burst equation as described under "Experimental Procedures."

The effects of Be^{2+} in the RT-catalyzed polymerase reaction were initially tested in the presence of 100 μ*M* dTTP and 2 m*M* Mg^{2+}. As shown in Table I, adding Be^{2+} ions produced an increase of the single turnover rate constant (k_{obs}) at concentrations in the range of 5–100 μ*M*, while exerting an inhibitory effect at millimolar concentrations. Pre-steady state kinetic analysis of the polymerization reaction carried out in the presence of 2 m*M* Mg^{2+} confirmed that Be^{2+}/dTTP was a better substrate than Mg^{2+}/dTTP. The obtained k_{pol} and K_d values for the incorporation of dTTP (complexed with Be^{2+}) were 20.7 ± 2.0 s^{-1} and 13.1 ± 4.0 μ*M*, respectively. While the apparent nucleotide affinity remained unchanged, the catalytic rate constant is increased twofold when Be^{2+} ions were present. In contrast, an inhibitory effect was observed at high $[Be^{2+}]$, which was

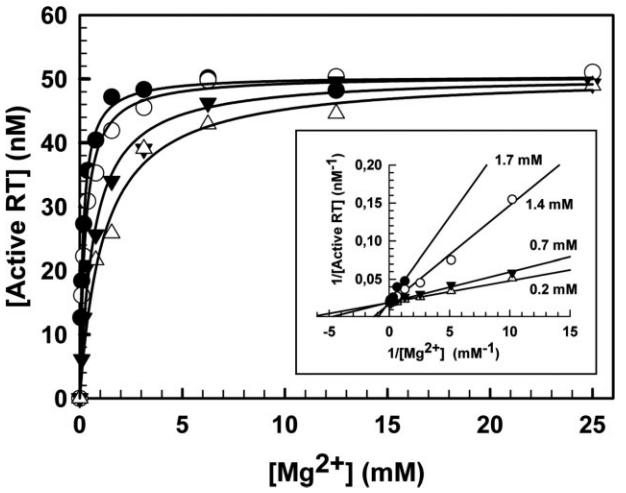

Figure 6

Inhibitory effects of Be^{2+} on the formation of a competent RT polymerase complex. Active RT concentrations ([RT/DNA/dNTP·Mg^{2+}/Mg^{2+}]) were determined from the burst amplitudes of the incorporation reactions carried out as described under "Experimental Procedures," but in the presence of 200 μM dTTP and varying concentrations of Mg^{2+}. Solid lines represent the best fit of the data obtained from experiments carried out in the presence of Be^{2+} at 0.2 mM (△), 0.7 mM (▼), 1.4 mM (○), and 1.7 mM (●). Free Be^{2+} concentrations in those assays were estimated at <5 μM, 0.5 mM, 1.2 mM, and 1.5 mM, respectively, assuming a K_d of 2.4 × 10^{-8} M for the Be^{2+}/dNTP complex.[30] The apparent K_d values obtained for Mg^{2+} binding to the RT complex in the presence of Be^{2+} at total concentrations of 0.2, 0.7, 1.4, and 1.7 mM were 164.1 ± 9.2 μM, 257.7 ± 20.9 μM, 682.4 ± 59.9 μM, and 691.2 ± 171.0 μM, respectively. Inset: double-reciprocal plot of the data.

detected as a reduction of the burst amplitude in the pre-steady state kinetic analysis. As shown in Figure 6, Mg^{2+} and Be^{2+} behave as competitive inhibitors for binding to site A. Therefore, Be^{2+} binding results in the inactivation of the catalytic polymerase complex. These experimental results are in agreement with the MD simulations obtained with the different complexes containing Be^{2+} ions, and support the functional distinction between metal sites A and B.

DISCUSSION

Metal ions with the right size and the right coordination geometry for nucleophilic attack facilitate the proper alignment of the catalytic residues and the nucleic acid substrate, thereby enhancing substrate recognition and catalytic specificity.[31] Current models for DNA polymerization are based on the comparison of binary (polymerase and DNA) and ternary (polymerase, template-primer DNA duplex, and dNTP at the polymerase active site) complexes. According to available models for HIV-1 RT, nucleotide binding to polymerase–DNA binary complexes involves a conformational change in which the "fingers" rotate from an "open" conformation to the "closed" state seen in the ternary complex. Our MD simulations based on the crystal structures of HIV-1 RT binary[25] and ternary complexes[15] show that upon binding of Mg^{2+}/dNTP, there is relatively large conformational transition that involves the movement of the "fingers" subdomain towards the "thumb" subdomain. The largest motion within the "fingers" subdomain affects the β3-β4 hairpin loop that bends over the "palm" subdomain forming an open ternary complex.

Binding of Mg^{2+} in metal site A (catalytic site) is required to obtain an RT which is catalytically competent for DNA polymerization. The presence of Mg^{2+} at the catalytic site is crucial for coordination with the 3′-OH found at the primer terminus and the nonbridging oxygen of the α-phosphate. Those interactions appear to be critical to maintain the 3′-OH and the α-phosphorus within an appropriate distance for nucleophilic attack. MD simulations show that the transition from a catalytically noncompetent open ternary complex to the catalytically competent "closed" conformation of the polymerase involves slight conformational changes, but significant rearrangements of the side-chains at the RT polymerase active site, particularly evident at the tip of the β3-β4 hairpin loop. This transformation could be identified as the rate-limiting noncovalent transition that precedes the formation of the transition state.[13]

The results obtained with HIV-1 RT are consistent with structural studies and MD simulations carried out with mammalian DNA polymerase β.[26,32] As in HIV-1 RT, conformational changes affecting DNA polymerase β involve the closing of the "thumb" subdomain as a consequence of Mg^{2+} binding at the catalytic site. Largest motions affect α-helix N,[26] within the "thumb" subdomain and away from the triphosphate moiety of the incoming dNTP. From a structural point of view, these changes are different from those observed with HIV-1 RT, whose largest movements occur within the β3-β4 hairpin loop while accommodating the incoming Mg^{2+}/dNTP in its binding site. The β3-β4 hairpin loop contains residues such as Lys-65 and Arg-72 whose side-chains make important hydrogen bonds with the incoming dNTP.[15] In addition, the β3-β4 hairpin loop also plays a relevant role in resistance to nucleoside analogue inhibitors of HIV-1 RT.[33]

The distinct properties of sites A and B have been probed with Be^{2+} ions. Although Be^{2+} has been identified as a relatively weak inhibitor of DNA polymerization reactions catalyzed by retroviral RTs,[16,29] it may affect the accuracy of DNA polymerization, as shown for avian myeloblastosis virus RT using homopolymeric template-primers as substrates.[7,16] Despite the tetrahedral coordination of Be^{2+}, our data show that Be^{2+}/dNTP are good substrates of the polymerization reaction. However, when Be^{2+} substitutes for Mg^{2+} at the catalytic site, the RT polymerase activity is inhibited due

to the loss of the critical interactions with the primer terminus and the incoming dNTP, that results in an increase of the nucleophilic attack distance that goes up to over 4.7 Å. Current models to explain the structural basis of DNA polymerase fidelity involve an induced-fit mechanism that includes both a global movement of the "fingers" subdomain upon substrate binding and subtle changes in the active site for metal ion coordination. According to this proposal, there are a number of possible check points for proper geometric alignment during nucleotide insertion by polymerases.[13] Our MD simulations revealed that the base pairing established upon binding of Mg^{2+}/dNTP remains stable along the 10-ns trajectory. Although these data suggest that a critical fidelity checkpoint occurs before the catalytically competent DNA polymerase complex is formed, further studies will be necessary to identify all relevant fidelity check points in DNA polymerization reactions catalyzed by HIV-1 RT or other DNA polymerases.

ACKNOWLEDGMENTS

We thank the CIEMAT (Madrid) for generous allowances of computer time on their SGI servers.

REFERENCES

1. Patel PH, Loeb LA. Getting a grip on how DNA polymerases function. Nature Struct Biol 2001;8:656–659.
2. Bebenek K, Kunkel TA. Functions of DNA polymerases. Adv Prot Chem 2004;69:137–165.
3. Ollis DL, Brick P, Hamlin R, Xuong NG, Steitz TA. Structure of large fragment of *Escherichia coli* DNA polymerase I complexed with dTMP. Nature 1985;313:762–766.
4. Kohlstaedt LA, Wang J, Friedman JM, Rice PA, Steitz TA. Crystal structure at 3.5 Å resolution of HIV-1 reverse transcriptase complexed with an inhibitor. Science 1992;256:1783–1790.
5. Beese LS, Steitz TA. Structural basis for the 3′-5′ exonuclease activity of *Escherichia coli* DNA polymerase I: a two metal ion mechanism. EMBO J 1991;10:25–33.
6. Steitz TA, Smerdon SJ, Jäger J, Joyce CM. A unified polymerase mechanism for nonhomologous DNA and RNA polymerases. Science 1994;266:2022–2025.
7. Sirover MA, Loeb LA. Infidelity of DNA synthesis *in vitro*: screening for potential metal mutagens or carcinogens. Science 1976; 194:1434–1436.
8. Beckman RA, Mildvan AS, Loeb LA. On the fidelity of DNA replication: Manganese mutagenesis in vitro. Biochemistry 1985;24: 5810–5817.
9. Snow ET, Xu LS, Kinney PL. Effects of nickel ions on polymerase activity and fidelity during DNA replication *in vitro*. Chem-Biol Interact 1993;88:155–173.
10. Cases-González CE, Gutiérrez-Rivas M, Menéndez-Arias L. Coupling ribose selection to fidelity of DNA synthesis–the role of Tyr-115 of human immunodeficiency virus reverse transcriptase. J Biol Chem 2000;275:19759–19767.
11. Batra VK, Beard WA, Shock DD, Krahn JM, Pedersen LC, Wilson SH. Magnesium-induced assembly of a complete DNA polymerase catalytic complex. Structure 2006;14:757–766.
12. Showalter AK, Tsai M-D. A reexamination of the nucleotide incorporation fidelity of DNA polymerases. Biochemistry 2002;41:10571–10576.
13. Joyce CM, Benkovic SJ. DNA polymerase fidelity: kinetics, structure and checkpoints. Biochemistry 2004;43:14317–14324.
14. Bakhtina M, Lee S, Wang Y, Dunlap C, Lamarche B, Tsai M-D. Use of viscogens, dNTPαS, and rhodium(III) as probes in stopped-flow experiments to obtain new evidence for the mechanism of catalysis by DNA polymerase β. Biochemistry 2005;44: 5177–5187.
15. Huang H, Chopra R, Verdine GL, Harrison SC. Structure of a covalently trapped catalytic complex of HIV-1 reverse transcriptase: implications for drug resistance. Science 1998;282:1669–1675.
16. Sirover MA, Loeb LA. Metal-induced infidelity during DNA synthesis. Proc Natl Acad Sci USA 1976;73:2331–2335.
17. Boretto J, Longhi S, Navarro J-M, Selmi B, Sire J, Canard B. An integrated system to study multiply substituted human immunodeficiency virus type 1 reverse transcriptase. Anal Biochem 2001;292: 139–147.
18. Matamoros T, Deval J, Guerreiro C, Mulard L, Canard B, Menéndez-Arias L. Suppression of multidrug-resistant HIV-1 reverse transcriptase primer unblocking activity by α-phosphate-modified thymidine analogues. J Mol Biol 2005;349:451–463.
19. Kati WM, Johnson KA, Jerva LF, Anderson KS. Mechanism and fidelity of HIV reverse transcriptase. J Biol Chem 1992;267:25988–25997.
20. Menéndez-Arias L. Studies on the effects of truncating α-helix E' of p66 human immunodeficiency virus type 1 reverse transcriptase on template-primer binding and fidelity of DNA synthesis. Biochemistry 1998;37:16636–16644.
21. Case DA, Darden T, Cheatham TE, III, Simmerling CL, Wang J, Duke RE, Luo R, Merz KM, Wang B, Pearlman DA, Crowley M, Brozell S, Tsui V, Gohlke H, Mongan J, Hornak V, Cui G, Beroza P, Schafmeister C, Caldwell JW, Ross WS, Kollman PA. AMBER 8. San Francisco, California: University of California; 2004.
22. Cieplak P, Cornell WD, Bayly CY, Kollman PA. Application of the multimolecule and multiconformational RESP methodology to biopolymers: charge derivation for DNA, RNA and proteins. J Comput Chem 1995;16:1357–1377.
23. Frisch MJ, Trucks GW, Schlegel HB, Scuseria GE, Robb MA, Cheeseman JR, Montgomery JA, Jr, Vreven T, Kudin KN, Burant JC, Millam JM, Iyengar SS, Tomasi J, Barone V, Mennucci B, Cossi M, Scalmani G, Rega N, Petersson GA, Nakatsuji H, Hada M, Ehara M, Toyota K, Fukuda R, Hasegawa J, Ishida M, Nakajima T, Honda Y, Kitao O, Nakai H, Klene M, Li X, Knox JE, Hratchian HP, Cross JB, Bakken V, Adamo C, Jaramillo J, Gomperts R, Stratmann RE, Yazyev O, Austin AJ, Cammi R, Pomelli C, Ochterski JW, Ayala PY, Morokuma K, Voth GA, Salvador P, Dannenberg JJ, Zakrzewski VG, Dapprich S, Daniels AD, Strain MC, Farkas O, Malick DK, Rabuck AD, Raghavachari K, Foresman JB, Ortiz JV, Cui Q, Baboul AG, Clifford S, Cioslowski J, Stefanov BB, Liu G, Liashenko A, Piskorz P, Komaromi I, Martin RL, Fox DJ, Keith T, Al-Laham MA, Peng CY, Nanayakkara A, Challacombe M, Gill PMW, Johnson B, Chen M, Wong W, Gonzalez C, Pople JA. Gaussian 03. Wallingford, CT, USA: Gaussian; 2004.
24. Pavlov M, Siegbhan PEM, Sandström M. Hydration of beryllium, magnesium, calcium and zinc ions using density functional theory. J Phys Chem A 1998;102:219–228.
25. Ding J, Das K, Hsiou Y, Sarafianos SG, Clark AD, Jr, Jacobo-Molina A, Tantillo C, Hughes SH, Arnold E. Structural and functional implications of the polymerase active site region in a complex of HIV-1 RT with a double-stranded DNA template-primer and an antibody Fab fragment at 2.8 Å resolution. J Mol Biol 1998;284: 1095–1111.
26. Yang L, Arora K, Beard WA, Wilson SH, Schlick T. Critical role of magnesium ions in DNA polymerase β's closing and active site assembly. J Am Chem Soc 2004;126:8441–8453.
27. Shanbhag SM, Choppin GR. Thermodynamics of Mg and Ca complexation with AMP, ADP, ATP. Inorg Chim Acta 1987;138:187–192.

28. Goldschmidt V, Didierjean J, Ehresmann B, Ehresmann C, Isel C, Marquet R. Mg^{2+} dependency of HIV-1 reverse transcription, inhibition by nucleoside analogues and resistance. Nucleic Acids Res 2006;34:42–52.
29. Sabbioni E, Blanch N, Baricevic K, Serra M-A. Effects of trace metal compounds on HIV-1 reverse transcriptase. An in vitro study. Biol Trace Elem Res 1999;68:107–119.
30. Boukhalfa H, Lewis JG, Crumbliss AL. Beryllium(II) binding to ATP and ADP: potentiometric determination of the thermodynamic constants and implications for *in vivo* toxicity. BioMetals 2004; 17:105–109.
31. Yang W, Lee JY, Nowotny M. Making and breaking nucleic acids: two-Mg^{2+}-ion catalysis and substrate specificity. Mol Cell 2006; 22:5–13.
32. Arora K, Schlick T. In silico evidence for DNA polymerase-β's substrate-induced conformational change. Biophys J 2004;87:3088–3099.
33. Cases-González CE, Franco S, Martínez MA, Menéndez-Arias L. Mutational patterns associated with the 69 insertion complex of multi-drug-resistant HIV-1 reverse transcriptase that confer increased excision activity and high-level resistance to zidovudine. J Mol Biol 2007;365:298–309.